

Toshiharu Enomae · Yoon-Hee Han · Akira Isogai

## Z-Directional distribution of fiber orientation of Japanese and western papers determined by confocal laser scanning microscopy

Received: October 5, 2007 / Accepted: January 24, 2008 / Published online: April 16, 2008

**Abstract** Confocal laser scanning microscopy was applied to visualize inside fibers stained with a fluorescent dye, and the fiber orientation distribution in the thickness direction was determined by image analysis from optically sliced images. Fiber orientation angle and anisotropy were determined by the fast Fourier transform method, which holds advantages over the conventionally applied Hough transform with regard to evaluation of fiber width-weighted contribution and intrafiber segmental contribution. An orthogonally layered Japanese paper handmade by the flow-sheet forming method resulted in a clear change of fiber orientation angle from 0° to 90°. Machine-made wood-containing printing paper showed the highest anisotropy, while copier paper showed a low anisotropy. Thick papers like the wood-free paperboard and recycled packaging board showed that the maximum measured thickness was about 150  $\mu\text{m}$ . The depth limit to detect fluorescence was considered to depend on the apparent density of the paper and the light absorption character of the fibers.

**Key words** Confocal laser scanning microscopy · Fiber orientation · Handmade paper · Washi · Fourier transform

### Introduction

In the papermaking industry, the use of innovative technologies such as the lamination of paper with other novel

materials and embedding of electronic microchips will become more common in the near future. These new types of paper products will go outside the reach of the conventional planer sheet structure and must be dealt with as a three-dimensional bulk structure. Therefore, analytical techniques that consider the three-dimensional structure of paper are predicted to become increasingly important. For this purpose, several techniques have been established. Mechanical slicing of paper with a microtome to make cross sections is a reliable but time-consuming method. Thin cross-sectional slices made so can be observed with an optical microscope. Developmentally, consecutive smooth cross sections of epoxy-embedded coating layers after successive grinding and polishing were obtained and reconstructed as a three-dimensional representation to visualize pigment particles and pores.<sup>1</sup> Recently, the focused ion beam has emerged in place of the microtome to make intact cross sections.<sup>2</sup>

Fiber orientation is one of the major parameters that dominate the physical properties of paper. For example, curl occurs when paper is moistened. The curl axis is usually consistent with the fiber orientation axis. However, fiber orientation, per se, does not cause curl, but the two-sided nature or transverse variation of components or structural parameters including fiber orientation causes it. Thus, the way in which fiber orientation distributes in the transverse direction (z-direction) is worth measuring as one of the paper structural parameters to predict three-dimensional deformation. Actually, a flow of a fiber suspension induces fiber orientation on a forming screen, and its degree has a distribution.<sup>3,4</sup>

According to a survey of traditional handmade paper like *washi* (Japanese paper) and *hanji* (Korean paper), it was found that bast fibers tend to be oriented in the case of *washi* more remarkably than conventional machine-made papers. This is because a fiber flow on a slanted forming screen consisting of bamboo splints woven together with silk threads, corresponding to a “forming wire” in the modern papermaking industry, during dehydration results in evident fiber orientation as observed for the flow sheet forming. If this principle is used the other way, fiber orienta-

T. Enomae (✉) · Y.-H. Han<sup>1</sup> · A. Isogai  
Paper Science Laboratory, Department of Biomaterial Sciences,  
Graduate School of Agricultural and Life Sciences, The University  
of Tokyo, 1-1-1 Yayoi, Bunkyo-ku, Tokyo 113-8657, Japan  
Tel. +81-3-5841-8199; Fax +81-3-5841-5271  
e-mail: enomae@psl.fp.a.u-tokyo.ac.jp

*Present address:*

<sup>1</sup>National Archives and Records Service, Daejeon 302-701, Republic of Korea

Part of this study was presented at the 54th Annual Meeting of the Japan Wood Research Society, Sapporo, Japan, August 2004

tion can be a physical basis to evaluate the effects of the motions of a mould (a wooden frame holding the forming screen) in the process of hand-making of cultural paper.<sup>5</sup> Other than evaluation of hand-making processes, information on fiber orientation distribution of a repair paper in the thickness direction should be useful to predict deformation of the repair paper over time after repairing.

Regardless of the sheet-forming tool (machine or hand), fiber orientation is one of the most important factors of paper properties and its distribution in the thickness direction plays an important role for deformation of the paper by both quick and slow environmental changes. To analyze the fiber orientation distribution, a representative conventional technique is the tape-stripping method. In this method, an adhesive tape is stuck on a paper surface; when the tape is ripped, a fiber layer with a certain thickness is removed together with the tape. The thickness and fiber orientation of the layer is measured to determine fiber orientation parameters as a function of the depth from the paper surface. Abe and Sakamoto<sup>6</sup> applied the tape-stripping method to separate thin layers from a whole sheet and measured Fraunhofer diffraction using a laser beam for fiber orientation. They confirmed that the angle-dependent distribution of optical density of the diffraction pattern recorded on the photographic film was in good agreement with fiber orientation distribution measured by another method and showed the characteristic fiber orientation distributions in the thickness direction for a shaking wire machine and a high speed machine, respectively. As well, Erikkila et al.<sup>7</sup> applied the tape-stripping method to split a sheet to 10 to 12 individual layers to determine fiber orientation angle and the anisotropy for each layer. The method for establishing the magnitude and direction of fibers in images taken with a video camera was image analysis using a Sobel operator-based procedure. Although such local filtering operator-based procedures are excellent to accomplish a quick operation, thick fibers are not weighted depending on their fiber width because only edges are detected sensitively by those filtering operators.

In the tape-stripping method, fiber breakage and pullout is inevitable and there is no guarantee that the layer thickness is uniform. A novel technique employed as an alternative in the present work is confocal laser scanning microscopy. The confocal system provides optical (non-mechanical) slicing, which solves the problems typical of mechanical layering, although sufficient precision is restricted within reach of the emitted light from fibers. Sliced layer images are obtained directly and are easily

subjected to image analysis. As an image analysis technique, Xu et al.<sup>8</sup> applied the Hough transform to detect fiber edges in pioneering work to acquire the index and angle of fiber orientation from confocal images. However, this popular method includes several problems in determination of fiber orientation. Only two edge lines are detected by the Hough transform for one fiber whether the fiber is thick or thin as well as the Sobel operator. In addition, curved fibers tend to be excluded from orientation calculation when the segments constituting one fiber are short, although each segment contributes to its tangential direction depending on its length. Therefore, in this work, a fast Fourier transform (FFT)-based algorithm was applied to determine fiber orientation parameters. The validity of the FFT method to evaluate fiber orientation was proved by Yuhara et al.<sup>9</sup> with the result obtained by applying it to a soft X-ray microdiagram of a paper sheet. This technique was extended to the three-dimensional fiber orientation of paper in our research.

## Experimental

### Samples

Five paper samples were used. Table 1 lists these samples with basis weight, thickness, and apparent density. The orthogonally layered Japanese paper was manufactured by Mr. Makoto Numata, a craftsman of Mino City, Gifu Prefecture. He produces the paper called *sai* by layering two thin sheet plies orthogonally to give one finished sheet of paper with improved dimensional stability. The other paper samples are commercially available machine-made papers.

Two test pieces measuring about 20 × 20 mm were taken from each sample. They were soaked in a 0.02% ethanolic solution of acridine orange, which is a fluorescent dye to stain pulp fibers. Each test piece was placed on a slide glass and covered with a cover glass. Then a drop of aniline was put on its corner or edge to allow it to penetrate the sample spontaneously to the other end, leaving as few air bubbles as possible. As an impregnation liquid in the case of pulp fibers, aniline was selected because its refractive index is 1.58, which is close to that of pulp fibers ranging between 1.57 and 1.60. A light beam does not refract at an interface between substances with equal refractive indices, but passes straight. Even a porous material like paper appears transparent when such a liquid fills its inside pores. Note that

**Table 1.** Paper samples used in this study

Paper	Basis weight (g/m <sup>2</sup> )	Thickness (μm)	Apparent density (kg/m <sup>3</sup> )
Orthogonally layered Japanese paper	24	55	440
Wood-containing D-grade printing paper	51	87	590
Copier paper, 100% recycled	64	96	660
Wood-free paperboard	155	167	930
Packaging paperboard, 100% recycled	365	453	810

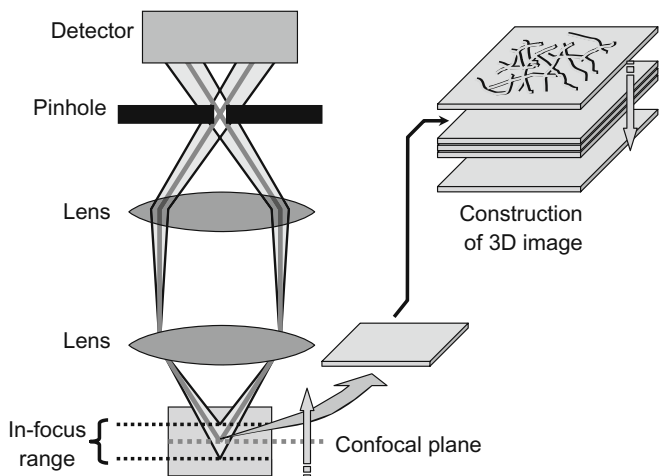


**Fig. 1.** Acquisition of three-dimensional image by confocal laser scanning microscopy (CLSM)

aniline is toxic and care must be taken not to touch it or inhale its vapor.

### Microscope conditions

A confocal laser scanning microscope (CLSM) LSM 510 with an upright body (Axioplan 2, Carl Zeiss, Germany) was used. As Fig. 1 shows, functions characteristic of this type of optical microscope to obtain three-dimensional (3D) images are optical slicing in the transverse direction by the confocal system and the intense power of laser beams to compensate for the resultant insufficient illumination. The term “confocal” means collecting light exclusively from a single plane in focus with a pinhole that eliminates light reflected from planes other than the focal plane. Laser beams fall on the front of a sample, and then reflect and enter the detector to provide a fluorescence image. The lenses used were a 10× objective and a 10× ocular to observe the sample at 100× magnification.

Sample observation used laser irradiation at 488 nm and optical filtering to restrict detection of light to fluorescence at about 512 nm that was emitted by fibers stained with acridine orange. The dimensions of the acquired images were  $0.92 \times 0.92$  mm at a resolution of  $512 \times 512$  pixels. Confocal plane thickness was  $5 \mu\text{m}$  for paper and  $8 \mu\text{m}$  for paperboard. The number of optical slices was 21 to 29 for one location and three to five locations were measured to average fiber orientation parameters at each depth.

Paper thickness measured by this CLSM method is comparable with that measured by the micrometer method, because the clamping pressure that develops between a cover glass and a slide glass is of the same order as that exerted by the micrometer platen. The clamping pressure  $P$  for the CLSM method depends on the surface tension  $\gamma$  of the liquid and the distance  $d$  between the cover and slide glasses.  $P$  is defined as  $2\gamma/d$ .  $\gamma$  of aniline is  $42.5$  mN/m. If  $d$  is assumed to be  $100 \mu\text{m}$ ,  $P$  is calculated to be  $85$  kPa, which is equivalent to  $P$  specified in the standard<sup>10</sup> for measuring paper thickness ( $50$  or  $100$  kPa).

### Image analysis to determine fiber orientation properties

Acquired optically sliced layer images were analyzed to determine the angle and anisotropy with regard to fiber orientation. Two-dimensional FFT was applied to determine those parameters. Fiber orientation can, in principle, be defined as an angular distribution of a power spectrum as a result of the integration  $q(\theta)$  of a power spectrum  $P(r, \theta)$  in polar coordinates, as shown in Eq. 1, where  $r$  is the radius and  $\theta$  is the polar angle. In the actual calculation procedure adopted in this work, the images were binarized using a dynamic threshold method of a simple moving average. This was performed to correct the shading of images taken under nonuniform illumination that would frequently obscure the measurement of true fiber orientation.

$$q(\theta) = \sum_{r=0}^{N/2} P(r, \theta) \quad (1)$$

A two-dimensional Fourier transform inevitably produces irregular large powers only in the  $x$  and  $y$  axes in the frequency domain when the gray levels of the left and right edges and the top and bottom edges of the image differ greatly, because FFT assumes infinite repetitions of the image in those directions. This binarization process efficiently reduces this abnormally large power by assigning an almost identical number of pixels to black or white. In addition, this method of binarization can extract the edges of out-of-focus fibers located below in-focus top fibers even in completely out-of-focus images. The FFT was computed with these binary images to obtain the power spectra.

When mean amplitude values are determined for each value of angle  $\theta$ , each discrete frequency value of the Fourier coefficients in the  $X$ - $Y$  coordinates cannot be easily converted to the exact corresponding position in the polar coordinates. If one draws the radius of a given angle from the pole in the frequency domain, it would pass through only a few discrete positions. The interpolation was applied using four adjacent amplitude values. The procedure is detailed in the literature<sup>11</sup> and is summarized in the following way. In the polar coordinates, the amplitude of the Fourier coefficient was added in a radial direction from the pole and its mean  $\overline{A(\theta)}$  was determined for each value of angle  $\theta$  ranging from  $0^\circ$  to less than  $180^\circ$ . The closed curve combining  $\overline{A(\theta)}$  and  $\overline{A(\theta+180)} = \overline{A\theta}$  was approximated to an ellipse using FFT followed by inverse FFT after low-pass filtering. The maximum value  $a$ , value  $b$  in the direction crosswise to  $a$ , and the angle  $\alpha$ , that is,  $\theta$  when  $\overline{A(\theta)} = b$ , were adopted as the lengths of the major axis, minor axis, and the orientation angle for elliptic parameters, respectively. Consequently, the anisotropy and the fiber orientation degree are defined as  $a/b$  and  $\alpha$ , respectively.

For one particular sample, representative values of orientation angle and anisotropy should be determined. Sliced layer images at the same depth of the same sample were collected from several locations within the same sample sheet. The mean orientation angle and anisotropy are defined as the means of several orientation angle and anisotropy values, respectively, calculated from every image at

the same depth. However, there was a problem in calculating the mean orientation angle. Orientation angle is expressed a value between  $0^\circ$  and less than  $180^\circ$ . The angles of  $0^\circ$  and slightly less than  $180^\circ$  represent the almost the same orientation angle, but the mean angle is calculated to be about  $90^\circ$ . In order to avoid this misleading result, the overall calculation was devised. The overall orientation angle and anisotropy is defined as a single value calculated overall from accumulated amplitude values of Fourier coefficients at the same angle of every image at the same depth. The difference in the orientation angle and anisotropy made by the two calculation methods is shown in the results.

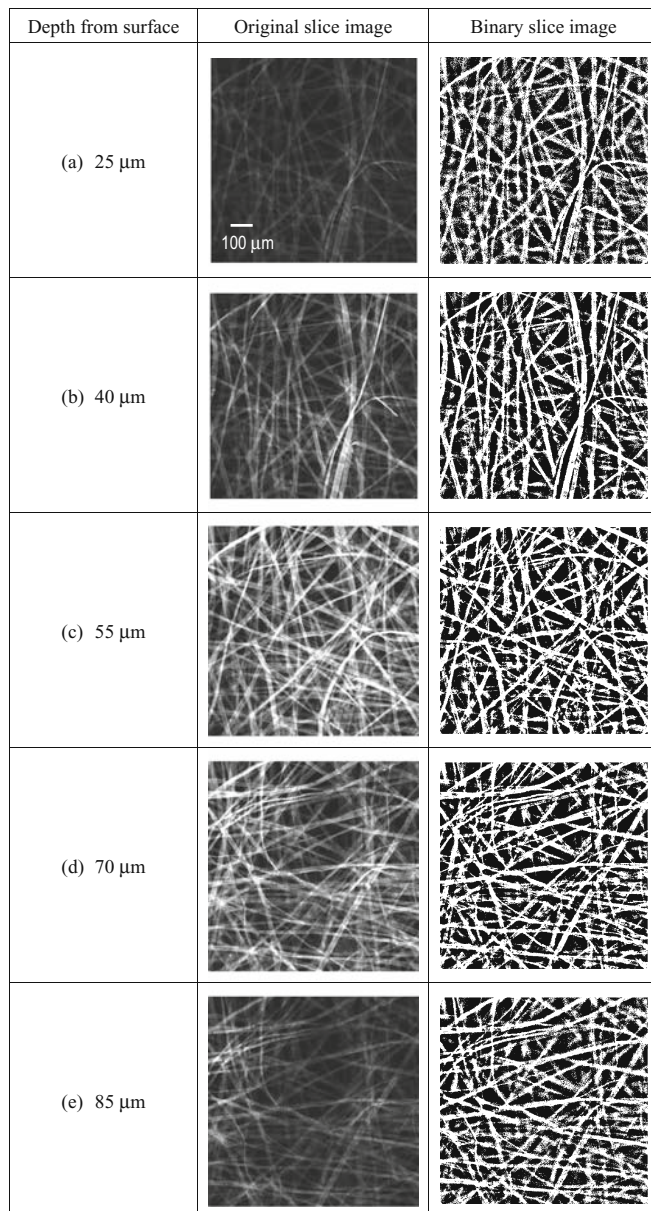
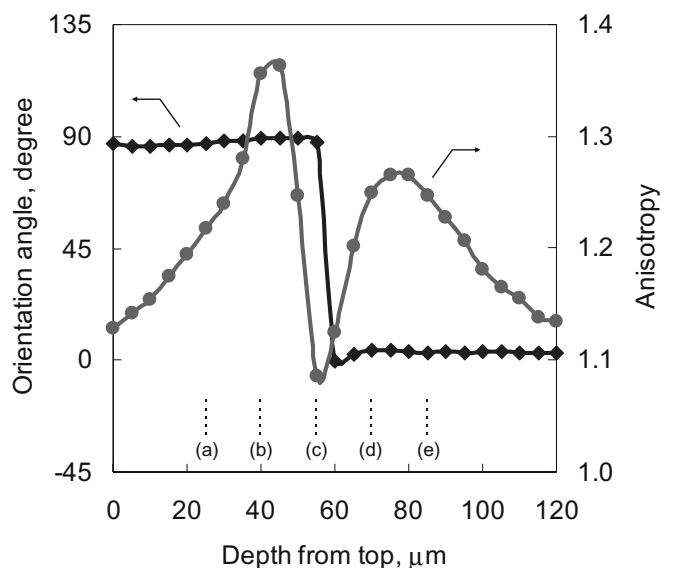


**Fig. 2a–e.** Original and binary confocal slice images of fibers in cross-lapped Japanese paper *sai*

## Results and discussion

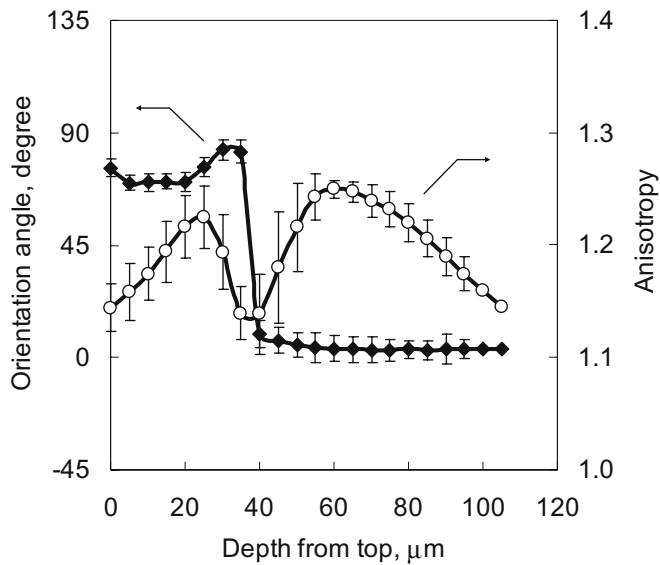
Figure 2 shows a set of optically sliced layer images for every 15  $\mu\text{m}$  in depth for the orthogonally layered Japanese paper from the top side of the first ply to the screen side of the second ply. In this context, the screen side corresponds to the wire side in the modern papermaking industry. The images shown are actually every third image from a series of 25 images taken for slices every 5  $\mu\text{m}$  apart. The fibers in the top two images (Fig. 2a, b) are oriented in the vertical direction of the image while those in the bottom (screen side) two images (Fig. 2d, e) are oriented in the horizontal direction. The central image (Fig. 2c) appears to include equal numbers of fibers oriented in both the vertical and horizontal directions. The orthogonally layered planes appear to be located near the image shown in Fig. 2c. The sliced layer images above that shown in Fig. 2a or below that shown in Fig. 2e gave very faint fiber shapes, probably because leak fluorescence emitted by fibers in adjacent planes was detected, even though there was practically no fibers in those actual confocal slices. The thickness of this sample was measured to be 55  $\mu\text{m}$  with a micrometer, which roughly corresponds to the difference in depth between images shown in Fig. 2a and Fig. 2e. For all of the sliced layer images, fiber orientation angle and anisotropy were calculated using FFT-based image analysis.

Figure 3 shows a calculated result of fiber orientation for one location of the orthogonally layered Japanese paper. The fiber orientation angle is consistently around  $90^\circ$  for the top half (55  $\mu\text{m}$  thick), and around  $0^\circ$  for the bottom half (65  $\mu\text{m}$  thick), which is consistent with the visual perception of the sliced layer images in Fig. 2. The thickness of this orthogonally layered paper is 55  $\mu\text{m}$ . Thus, outside this thickness, light reflected from the top or bottom surfaces is



**Fig. 3.** Orientation angle (diamonds, left axis) and anisotropy (circles, right axis) of fiber orientation for one location of cross-lapped Japanese paper. Dotted lines marked a to e correspond to depths of slice images shown in Fig. 2





**Fig. 4.** Mean orientation angle (*diamonds*, left axis) and mean anisotropy (*circles*, right axis) of fiber orientation for cross-lapped Japanese paper. Bars show 95% confidence intervals

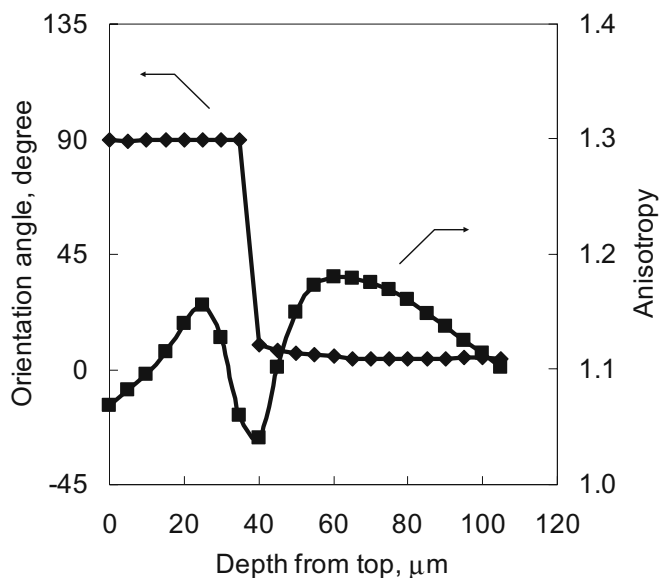


**Fig. 5.** Overall angle (*diamonds*, left axis) and anisotropy (*squares*, right axis) of fiber orientation for cross-lapped Japanese paper

considered to be detected faintly. The confocal mechanism does not guarantee complete limitation of light from out-of-focus planes. Then indistinct virtual images are detected about  $20\ \mu\text{m}$  above and below the paper surface layers. Therefore, the paper is measured to be about  $40\ \mu\text{m}$  thicker by the CLSM method than the thickness measured by the micrometer method. Rough papers like Japanese paper with fibers rising from the surface are measured to be about  $10\ \mu\text{m}$  thicker. The anisotropy is sensitive to the sheet structure change of orthogonal layering. At  $55\ \mu\text{m}$  from the top, the anisotropy was lower than 1.1. With this calculation process, anisotropies higher than 1.15 suggest strong fiber orientation while those lower than 1.10 imply almost random

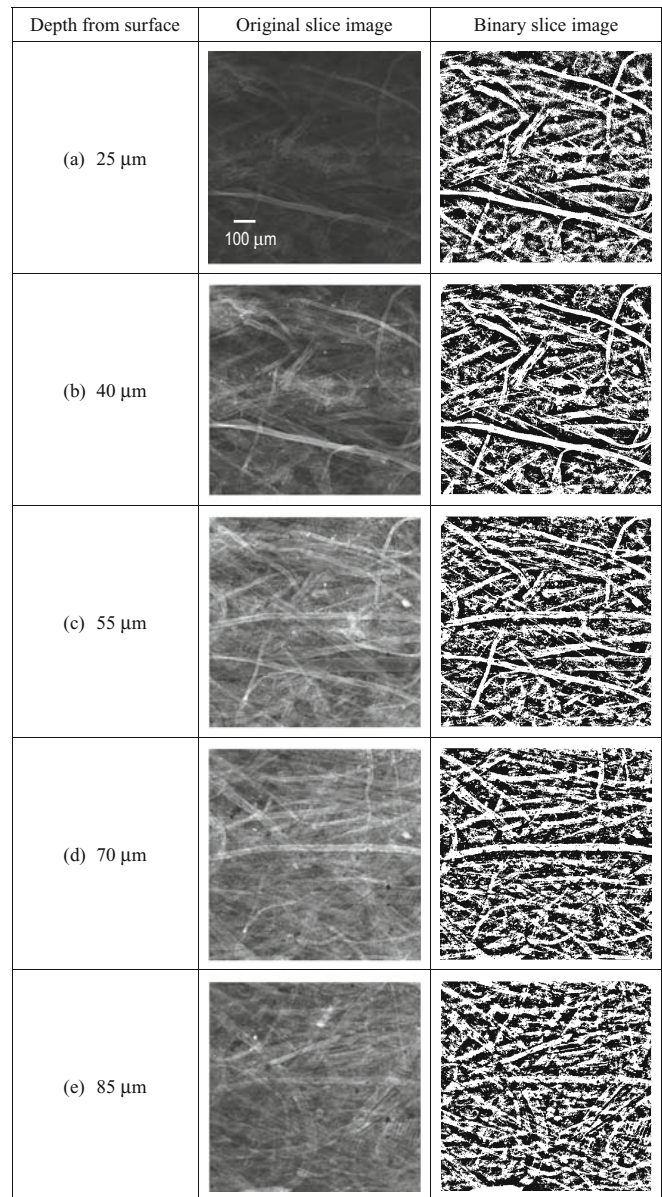


**Fig. 6a–e.** Original and binary confocal slice images of fibers in wood-containing paper

orientation. Thus, fiber orientation near the lapping plane was estimated to be random due to the mixture of fibers aligned in cross directions. This sheet has two peaks of anisotropy in the centers of the two respective plies.

Figure 4 shows the mean fiber orientation angle and anisotropy calculated from ten sets of sliced images for the orthogonally layered Japanese paper. Each set of images was shifted in the depth direction so that the angle change plane was between  $35$  and  $40\ \mu\text{m}$  in depth. There was no difficulty during this arrangement because every set of the sliced layer images had the plane exhibiting a clear orientation angle change. Figure 4 confirms that this orthogonally layered paper has the crosswise structure over the whole area and that the CLSM technique is feasible to determine the internal fiber orientation.

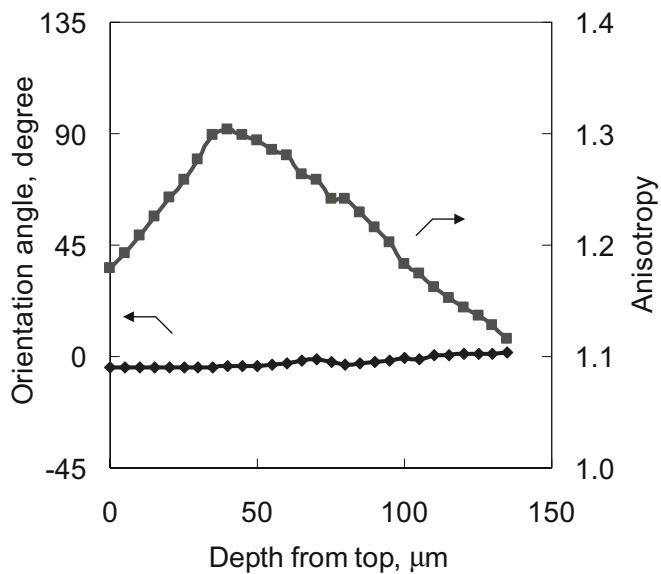


**Fig. 7.** Overall angle (diamonds, left axis) and anisotropy (squares, right axis) of fiber orientation for wood-containing paper

Figure 5 shows an overall fiber orientation angle and anisotropy of the orthogonally layered Japanese paper. The data for Fig. 4 are mean values of angle and anisotropy of all images at each depth. Therefore, 95% confidence intervals can be calculated, as shown in Fig. 4, from all the values. However, the data for Fig. 5 are single values of angle and anisotropy, and it is impossible to calculate 95% confidence intervals. This overall calculation means the large-area sampling that covers the sum of the imaged areas subjected to the analysis and permits determination of the true orientation angle. Overall anisotropies tend to be lower than the corresponding mean anisotropies. Overall anisotropies higher than 1.10 suggest strong fiber orientation while those lower than 1.05 imply almost random orientation.

Figure 6 shows a set of sliced layer images for wood-containing printing paper. Among machine-made paper samples used in this work, this wood-containing paper is likely to have the highest anisotropy. The fibers are observed to be orientated clearly in the machine direction, namely, the horizontal direction in the image. Figure 7 shows the overall angle and anisotropy of fiber orientation for the sample. The highest anisotropy reaches 1.30 across the thickness. The sliced layer with this anisotropy peak occurs toward the top surface, which is probably the wire side, considering that the wire side of paper is formed earlier than the top side, immediately after fibers contact the wire, causing more remarkable fiber orientation.

Figure 8 shows a set of sliced layer images for copier paper. Generally, copier paper is designed for less fiber orientation to prevent wrinkles that may occur around heating rolls that are installed in copying machines to fix toner. For the sliced layer images, fiber orientation is not discernible by eye. Figure 9 shows that the anisotropy is

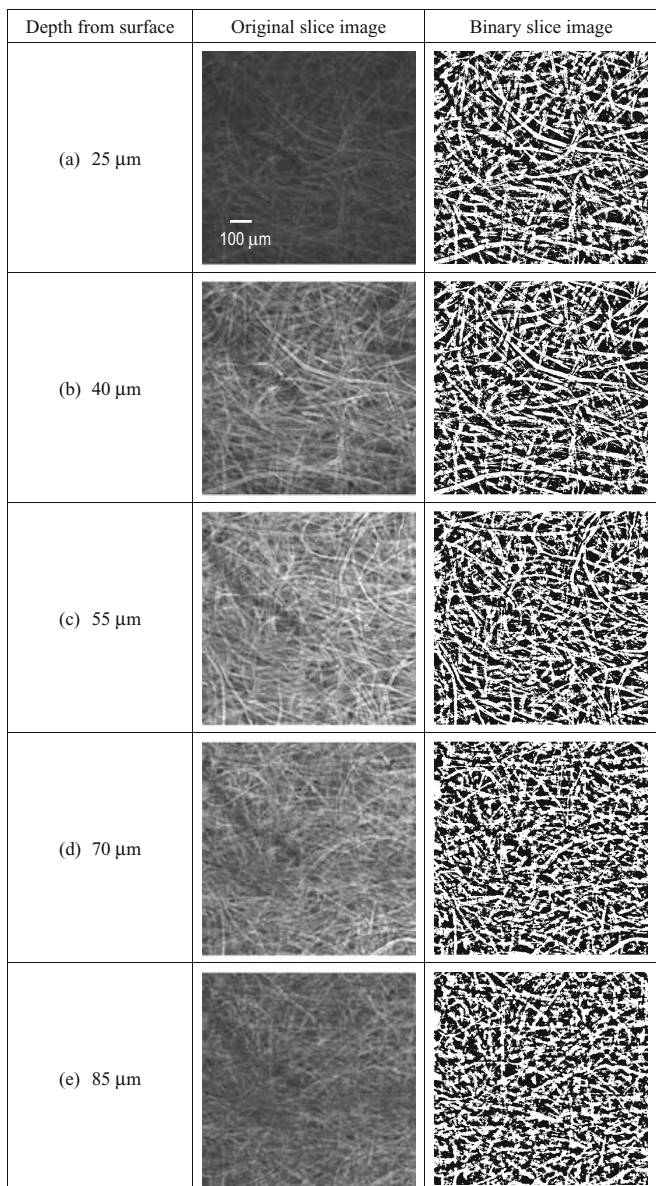


**Fig. 8a–e.** Original and binary confocal sliced layer images of copier paper

lower for the copier paper than any other paper samples used here.

Figures 10 and 11 show overall angle and anisotropy of fiber orientation for the wood-free paperboard and recycled packaging board, respectively. For the wood-free paperboard, the possible range of measured thickness was 152  $\mu\text{m}$  at the highest, although the actual thickness measured by micrometer was 167  $\mu\text{m}$ . Reflected light photographed in the sliced layer images near the last image at 152  $\mu\text{m}$  in depth is so faint that sliced layer images below this layer would not provide accurate analysis. Paper with very high density like this wood-free paperboard absorbs and scatters light reflected from a deep layer to a great extent. The results for the two paperboard samples suggest that internal structure analysis by CLSM is applicable for paper or paper-

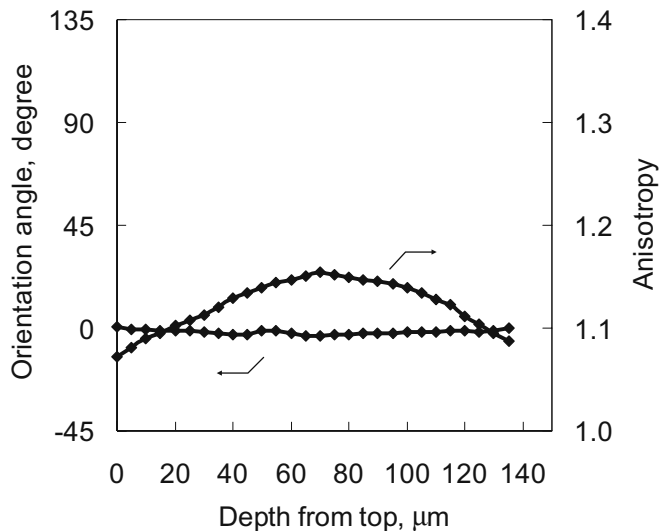


**Fig. 9.** Overall angle (diamonds, left axis) and anisotropy (diamonds, right axis) of fiber orientation for copier paper

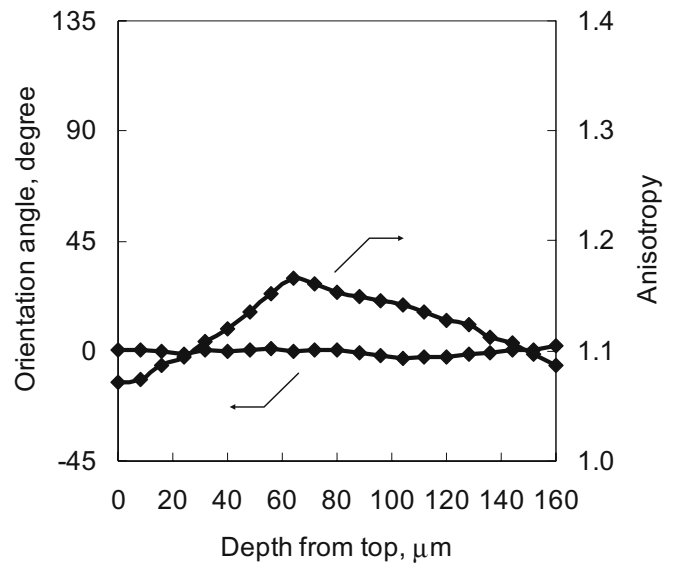


**Fig. 11.** Overall angle (diamonds, left axis) and anisotropy (diamonds, right axis) of fiber orientation for paperboard for paper container

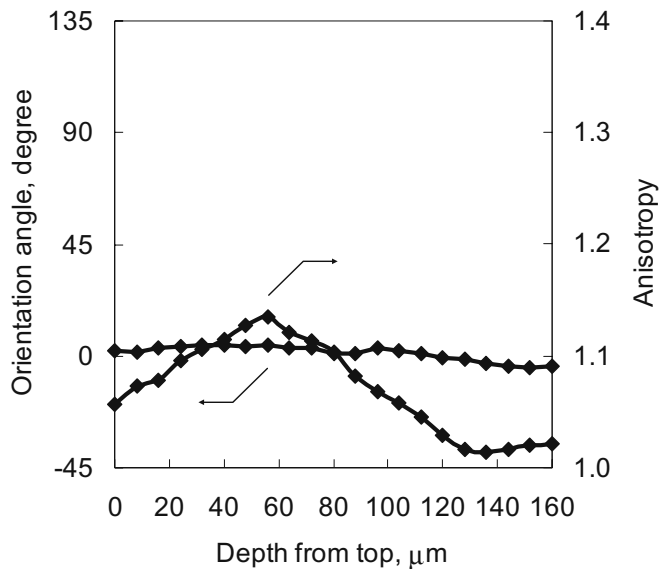


**Fig. 10.** Overall angle (diamonds, left axis) and anisotropy (diamonds, right axis) of fiber orientation for wood-free paperboard

board to a maximum depth of 150  $\mu\text{m}$ , although the actual depth depends on the apparent density. The packaging board had a higher maximum value of anisotropy than the wood-free paperboard. Below the sliced layer at 64  $\mu\text{m}$  deep, the anisotropy decreased with the depth for the same reason; namely, an insufficient amount of reflected light. In particular, dark gray fibers used in recycled paperboards tend to absorb emitted fluorescent light.

## Conclusions

Confocal laser scanning microscopy is a useful technique to examine the internal structure of paper or paperboard when

stained with acridine orange. The fiber orientation distribution in the thickness direction was determined by applying Fourier transform image analysis to every sliced layer image of paper. Fiber orientation angle and anisotropy were determined by the FFT method, which holds advantages over the Hough transform with regard to evaluation of fiber width-weighted contribution and intrafiber segmental contribution. Japanese handmade paper is known to have a strong orientation because flow of the fiber suspension orientates fibers during dehydration in flow-sheet forming. An orthogonally layered Japanese paper, a model of a structure with a clear change of fiber orientation at the orthogonally layered plane, resulted in a clear change of fiber orientation angle from  $0^\circ$  to  $90^\circ$  and two peaks of anisotropy in the two plies, respectively. This result demonstrates the validity of the CLSM method. For machine-made papers, the wood-containing printing paper showed the highest anisotropy, while the copier paper showed a low anisotropy presumably because copier paper is designed to be free of wrinkles during copying. Thick papers like the wood-free paperboard and recycled packaging board showed the possible range of measured thickness was about 150  $\mu\text{m}$ . Fluorescence emitted from fibers deeper than 150  $\mu\text{m}$  is too faint to be used for FFT-based image analysis, although the depth limit depends on the apparent density of the paper and the light absorption character of the fibers.

**Acknowledgments** The authors thank Mr. Makoto Numata for preparing orthogonally layered Japanese paper *sai*.

## References

- Chinga G, Helle T (2003) Three-dimensional reconstruction of a coating layer structure. *J Pulp Paper Sci* 29:119–122

2. Uchimura H, Kimura M (1998) A sample preparation method for paper cross-sections using a focused ion beam (in Japanese). *Sen'i Gakkaishi* 54:360–366
3. Niskanen K, Kajanto I, Pakarinen P (2001) Paper structure. In: Niskanen K (ed) *Paper physics. Papermaking Science and Technology Series*, vol 16. TAPPI, Atlanta, pp 37–47
4. Eguchi A, Sueoka Y, Kuragasaki M, Makino T (1993) Flow characteristics in a headbox and fiber orientation of paper (part 1). Flow characteristics in flow passage model (in Japanese). *Jpn TAPPI J* 47:398–406
5. Han Y-H, Enomae T, Isogai A, Yamamoto H, Hasegawa S, Song J-J, Jang S-W (2006) Traditional papermaking techniques revealed by fiber orientation in historical papers. *Stud Conserv* 52:267–276
6. Abe Y, Sakamoto S (1991) Measurement of the Z-direction profile of fiber orientation in paper by laser diffraction (in Japanese). *Jpn TAPPI J* 45:694–701
7. Erikkila AL, Pakarinen P, Odell M (1998) Sheet forming studies using layered orientation analysis. *Pulp Pap* 99:81–85
8. Xu L, Parker I, Filonenko Y (1999) A new technique for determining fibre orientation distribution through paper. 1999 International Paper Physics Conference Proceedings, TAPPI, Atlanta
9. Yuhara T, Hasuike M, Murakami K (1991) Fibre orientation measurement with the two-dimensional power spectrum of a high-resolution soft X-ray image. *J Pulp Pap Sci* 17:110–114
10. International Organization for Standardization (2005) ISO 534:2005 Paper and board determination of thickness, density and specific volume. International Organization for Standardization, Geneva
11. Enomae T, Han Y-H, Isogai A (2006) Nondestructive determination of fiber orientation distribution of paper surface by image analysis. *Nord Pulp Pap Res J* 21:253–259